Spectroscopic Characterization of Heme A Reconstituted Myoglobin

Randy W. Larsen,, David J. Nunez, Jason MacLeod, Andrew K. Shiemke*, Siegfried M. Musser, Hiep Hoa Nguyen, Mark R. Ondrias and Sunney I. Chan

RWL, JM, AKS, SMM, HHN, SIC. *Arthur Amos Noyes Laboratory of Chemical Physics, California Institute of Technology, Pasadena, California.*—DJN, MRO. *Department of Chemistry, University of New Mexico, Albuquerque, New Mexico*

ABSTRACT

The focus of this study was to examine the functional role of the unusual peripheral substitution of heme A. The effects of heme A stereochemistry on the reconstitution of the porphyrin have been examined in the heme A-apo-myoglobin complex using optical absorption and resonance Raman and electron paramagnetic resonance spectroscopies. The addition of one equivalent of heme A to apo-Mb produces a complex which displays spectroscopic signals consistent with a distribution of high- and low-spin heme chromophores. These results indicate that the incorporation of heme A into apo-Mb significantly perturbs the protein refolding.

INTRODUCTION

The respiratory systems of aerobic organisms contain a number of complex energy transducing proteins which ultimately couple electron transfer to the synthesis of ATP. The terminal step in this process involves an enzyme complex which catalyzes the reduction of O_2 utilizing electrons derived from the various substrates. Energy conservation is realized in the electron transfer from substrate to O_2 which is coupled to the vectorial transport of protons across a membrane barrier.

Cytochrome c oxidase, the terminal enzyme in the respiratory systems of aerobic eukaryotic organisms, is structurally and functionally unique among

* Current address: Department of Biochemistry, West Virginia University Medical School, Morgantown, WV 26506.

Address reprint requests to: Dr. Sunney I. Chan, Division of Chemistry and Chemical Engineering, California Institute of Technology, Pasadena, CA 91125.

Journal of Inorganic Biochemistry, 48, 21–31 (1992)
© 1992 Elsevier Science Publishing Co., Inc., 655 Avenue of the Americas, NY, NY 10010 0162-0134/92/$5.00

metalloproteins. This class of enzymes contain two heme A chromophores and two copper ions per minimal functional unit and catalyzes the reduction of dioxygen to water using electrons derived from ferrocytochrome c [see Ref. 1 for review]. Heme A contains distinctive peripheral substitutions with a vinyl group at position 4, a formyl group at position 8, a 1′-hydroxy-5′,9′,13′-trimethyl-4′,8′,12′-*trans,trans*-tetradecatrienyl group at position 2 and propionic acid groups at positions 6 and 7 [2]. In contrast, the most common porphyrin in biological systems is heme b. This chromophore contains vinyl substituents at the 2 and 4 positions and propionic acid side-chains at the 6 and 7 positions (See Fig. 1 for a diagram of the structures of heme A and heme b. The b-type heme active site performs a wide range of physiological functions including the reversible binding and activation of O_2 and is the prosthetic group of many heme proteins, including hemoglobins, myoglobins, peroxidases, catalases, and oxygenases.

The functional role of the unique peripheral substitutions of heme A relative to heme b has yet to be determined. Of specific interest is the apparent preference of terminal oxidases for heme A as the heme active sites in this class of enzymes. The formyl group of the low-potential cytochrome a in cytochrome c oxidase has been implicated as the site of redox-linked proton translocation in this enzyme based upon hydrogen bonding characteristics observed in the resonance Raman spectrum of the ferric and ferrous forms of the enzyme [3]. The lack of any direct experimental evidence, however, precludes direct association of this heme center with proton translocation. The functional significance of the isoprenoid chain at position 2 of the heme A macrocycle is also unknown. It has been generally assumed that the hydrophobic side-chain plays either a structural role in the orientation of heme A within the protein, or as an electron transfer "conduit" leading into or out of the heme site. The latter proposal appears unlikely since the side-chain is not highly conjugated. A more recent model has been proposed in which the side-chain is involved in proton translocation centered at cytochrome a_3 by directly coordinating to the heme group [4].

The focus of this study is to examine the extent to which the structure of the heme prosthetic group of cytochrome c oxidase influences the catalytic function of this class of enzyme. The effects of heme A stereochemistry on the reconsti-

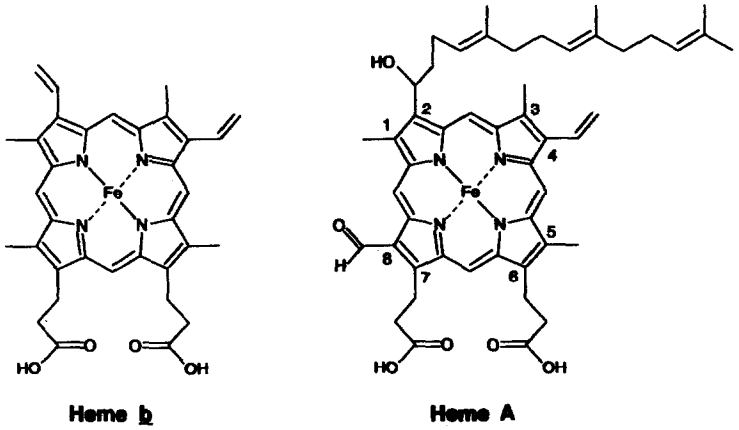

Heme b **Heme A**

FIGURE 1. Structural diagram of heme b (protoporphyrin IX) and heme A.

tution of the porphyrin have been examined in heme A-apo-myoglobin (apo-Mb) complex using optical absorption and resonance Raman and electron paramagnetic resonance spectroscopies. Apo-Mb has been chosen for this study because this protein has been well characterized and has been shown to be easily reconstituted with a variety of different porphyrin macrocycles [5–8]. In addition, early studies by Lemberg et al. [9] demonstrated that heme A reacts with protein-donated nitrogeneous ligands of a variety of proteins including albumins, apo-hemoglobin, and apo-Mb. The results obtained here show that heme A and apo-Mb form a 1:1 complex with spectroscopic signatures consistent with a distribution of high- and low-spin heme chromophores. These observations suggest that the incorporation of heme A into apo-Mb significantly perturbs the protein refolding.

MATERIALS AND METHODS

Cytrochrome c oxidase was prepared from bovine heart muscle according to the method of Hartzell and Beinert [10]. Heme A was isolated from purified cytochrome c oxidase by the procedure of Takemori and King [11] and stored at 197 K. Horse heart myoglobin (Sigma type I) was used without further purification.

Apo-myoglobin was prepared by the acid-butanone method of Teal [12]. Approximately 1 mg of horse heart myoglobin was dissolved in 2 mL deionized water and cooled to ice temperature. The solution pH was adjusted to pH2 using 1 N HCl. Cold butanone (5 mL) was then added to extract the native heme b. The apo-protein was then dialyzed against 100 volumes of 10 mM $NaHCO_3$ for 4 h and again with 100 volumes of 100 mM Tris, pH 6.5 for an additional 8 h with two changes of buffer. The apo-myoglobin was then centrifuged at 16,000 rpm for 30 min to remove aggregated protein. The extent of heme depletion was monitored using the intensity ratio of Soret to 280 nm absorption bands. It was determined that heme b removal was greater than 98%.

Heme A used for reconstitution was dissolved in a minimal volume of cold 0.1 N NaOH. The concentration of heme A was determined using $\varepsilon_{587} = 27\ mM^{-1}\ cm^{-1}$ for the corresponding heme A pyridine hemochrome [11]. The concentration of apo-Mb was determined using $\varepsilon_{280\ nm} = 15\ mM^{-1}\ cm^{-1}$ in 100 mM Tris, pH 6.5. Heme A was added slowly to the apo-Mb solution to give a final molar ratio of 2:1 heme A:apo-Mb. The resulting solution was incubated at 50°C for 30 min and subsequently placed on a Sephedex G-25 chromatography column (1×5 cm) equilibrated with 100 mM Tris (pH 6.5) to remove uncomplexed heme A. The heme A-apo-Mb complex could be stored at 5°C for several days without significant degradation. Considerable denaturation did occur following several cycles of freeze/thaw.

The fully reduced form of the heme A-apo-Mb complex was prepared by degassing approximately 1 mL of 20 μM complex (100 μM in the case of the resonance Raman studies) with five cycles of vacuum/Ar followed by the addition of a slight excess of solid sodium dithionite (Aldrich).

Heme A model compounds were prepared from a stock solution of ~ 1.5 mM heme A in DMSO. The concentration of heme A was determined using the heme A-pyridine hemochrome method described above. The high-spin heme A model complex was prepared by diluting an aliquot of the stock heme A solution

to 20 μM in DMSO. The corresponding low-spin heme A model complex was prepared by diluting an aliquot of the heme A stock solution in DMSO containing ~ 100 mM imidizole. The reduced forms of the high- and low-spin heme A model compounds were prepared by adding several grains of solid sodium dithionite to the given model complex which had been previously purged with Ar for 30 min.

Optical absorption spectra were obtained on an HP8452 diode array UV/Vis spectrometer or a Beckman DU-7 UV/Vis spectrometer interfaced to a personal computer. Resonance Raman spectra were recorded using instrumentation described elsewhere [13]. EPR spectra were recorded using a Varian E-line Century Series X-band spectrometer outfitted with an Oxford Instruments liquid He low-temperature cryostat.

RESULTS

The addition of heme A to a solution of apo-Mb produces a complex between the porphyrin and the apo-protein, as is evident from the optical titration of apo-Mb with heme A (Fig. 2). The titration data indicate that apo-Mb forms a 1:1 complex with heme A. In addition, heme A could not be dissociated with high detergent concentrations (2% Brij-35) or in the presence of a large excess of CN^- (as judged from size exclusion chromatography). The lack of heme A dissociation with high-detergent concentrations indicates that the observed binding of heme A to apo-Mb does not involve strictly hydrophobic interactions with the protein (i.e., heme A is not hydrophobically bound to the exterior of the protein but associated to the apo-Mb at or near the heme b binding site). In addition, the stability of the heme A-apo-Mb complex in the presence of excess CN^- further suggests that heme A is incorporated into the protein matrix.

The optical absorption spectra of ferric heme A bis-DMSO and ferric heme A bis-imidizole model complexes are compared with that of the heme A-apo-Mb complex in Figure 3. Previous studies have determined that the ferric heme A bis-DMSO complex is 6-coordinate and high-spin [14, 15]. The absorption spectrum of the ferric high-spin heme A bis-DMSO complex displays a Soret maximum at 410 nm with bands in the visible region at 544 nm, 600 nm, and 645 nm. The 6-coordinate, low-spin ferric heme A bis-imidizole complex shows a

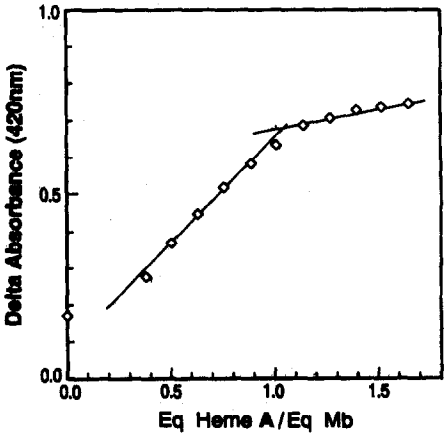

FIGURE 2. Optical titration of heme A with apo-Mb. Points were obtained by subtracting the absorption spectrum of a reference containing heme A in 100 mM Tris, pH 6.5, from the sample containing heme A and apo-Mb in the same buffer. Apo-protein concentration was 5 μM while the heme A stock solution was 1 mM. Sample volume was 1 mL in a 1 cm pathlength quartz cuvette.

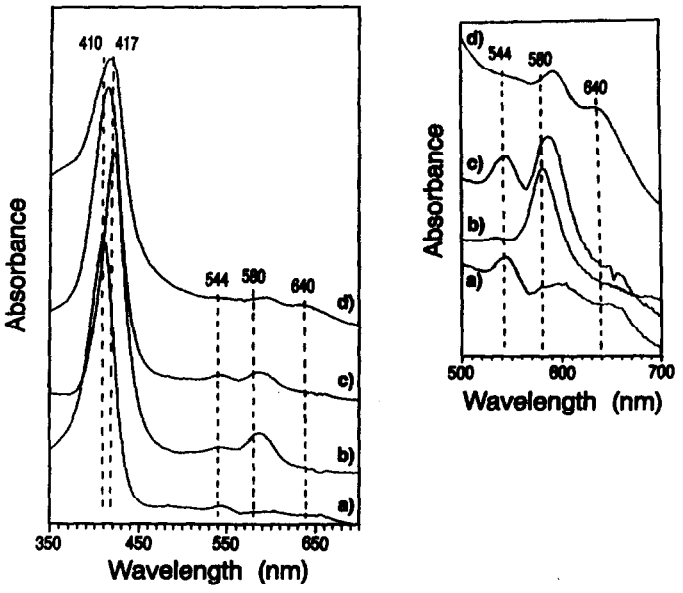

FIGURE 3. Optical absorption spectra of (a) ferric heme A bis-DMSO complex, (b) ferric heme A bis-imidizole complex in DMSO, (c) mathematical sum of the individual absorption spectra of the ferric heme A bis-DMSO and ferric heme A bis-imidizole complexes, and (d) ferric heme A-apo-Mb complex. The inset displays an expanded view of the visible region (500–700 nm). Sample concentration was 20 μM for the ferric heme A bis-DMSO and ferric heme A bis-imidizole complexes and 10 μM for the ferric heme A-apo-Mb complex. All spectra were obtained in a 1 cm pathlength quartz cuvette at room temperature.

Soret maximum at 424 nm and visible bands at 542 nm and 590 nm. The corresponding optical absorption spectra of the ferric heme A-apo-Mb (Fig. 3d) displays a Soret band maximum at 417 nm with additional bands in the visible region at 591 nm and 640 nm, which is similar to those previously reported by Lemberg et al. [9]. The absorption spectrum of the ferric heme A-apo-Mb complex is remarkably close to the spectra obtained from a 1:1 sum of the individual spectra from the ferric heme A bis-DMSO and ferric heme A bis-imidizole complexes (Fig. 3c).

Figure 4 gives a similar comparison of the optical absorption spectra of the ferrous heme A-apo-Mb complex (Fig. 4a) with that of the ferrous heme A bis-imidizole complex (Fig. 4b) and the ferrous heme A bis-DMSO complex (Fig. 4c) in DMSO. The ferrous heme A bis-DMSO and ferrous heme A bis-imidizole complexes both exhibit a Soret maximum near 436 nm. In addition, prominent bands are observed at 581 nm (ferrous heme A bis-DMSO complex) and 585 nm (ferrous heme A bis-imidizole complex) in the visible region. The ferrous heme A-apo-Mb complex exhibits a Soret band at 440 nm with an additional band in the visible region at 595 nm.

The high-frequency resonance Raman spectra of the ferric and ferrous heme A-apo-Mb complexes are shown in Figure 5a and 5b, respectively. The ferric heme A-apo-Mb complex displays Raman bands at 1372 cm^{-1} (ν_4), 1505 cm^{-1} (ν_3, 6-coordinate low-spin), 1490 cm^{-1} (ν_3, 5-coordinate high-spin), 1570 cm^{-1}

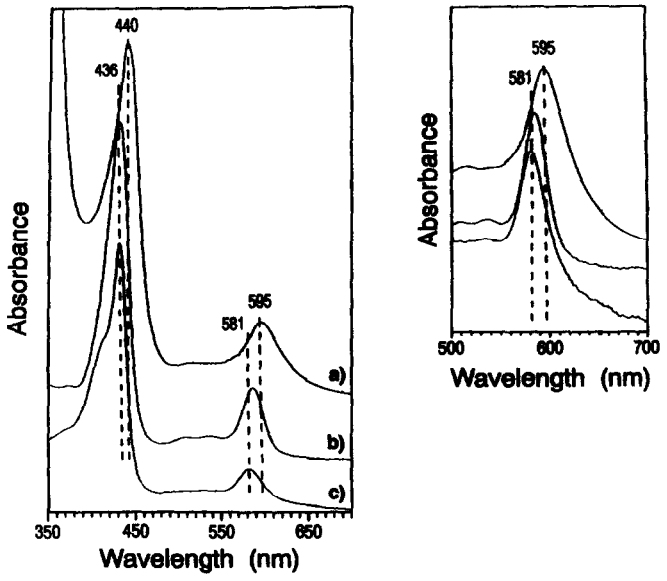

FIGURE 4. Optical absorption spectra of (a) ferrous heme A-apo-Mb complex, (b) ferrous heme A bis-imidizole complex in DMSO, and (c) ferrous heme A-bis-DMSO complex. Sample and spectral conditions are the same as in Figure 3.

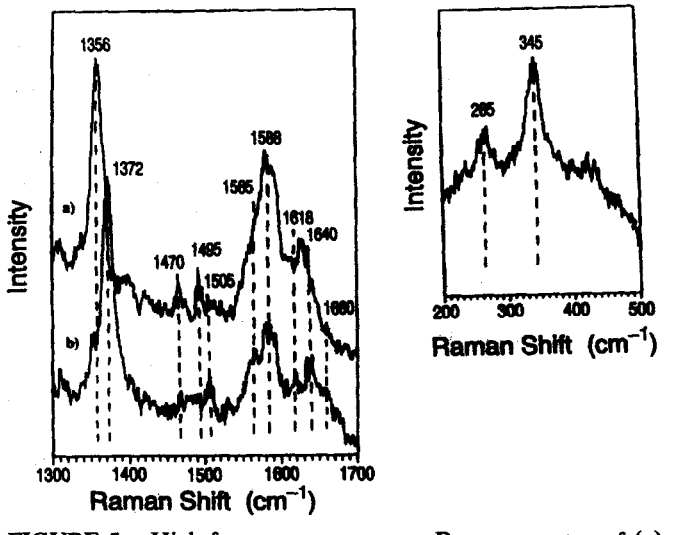

FIGURE 5. High-frequency resonance Raman spectra of (a) ferrous heme A-apo-Mb and (b) ferric heme A-apo-Mb complexes. The inset displays the low-frequency region of the ferrous heme A-apo-Mb complex. Sample concentration was 100 μM. Excitation frequency was 410 nm (0.3 mJ/pulse) for the ferric complex and 440 nm (0.8 mJ/pulse) for the ferrous complex.

(ν_2, high-spin), and 1588 cm^{-1} (ν_2, low-spin). The broad band centered at 1640 cm^{-1} may contain contributions from ν_{10} (1610 cm^{-1} for 5-coordinate high-spin and 1640 cm^{-1} for 6-coordinate low-spin) and $\nu_{C=O}$ whose position varies with both the metal spin- and oxidation-state as well as the solvent environment of the heme. The high-frequency resonance Raman spectrum of the ferrous heme A-apo-Mb complex displays vibrational bands at 1356 cm^{-1} (ν_4), 1470 cm^{-1} (ν_3, 6-coordinate low-spin), 1500 cm^{-1} (ν_3, 5-coordinate high-spin) and 1588 cm^{-1} (ν_2). The low-frequency resonance Raman spectrum of the ferrous heme A-apo-Mb complex is shown in the inset of Figure 5. The spectrum displays only two prominent vibrational bands at 265 cm^{-1} (ν_9) and 345 cm^{-1} (ν_8).

The EPR spectra of native Mb and the heme A-apo-Mb complex are shown in Figure 6a and 6b, respectively. Both species display resonances at $g = 6.0$ and $g = 2.0$. The resonances at $g = 4.35$ and $g = 2.2$ observed for the heme A-apo-Mb complex can be attributed to a small amount of adventitiously-bound Fe and Cu, respectively. All spectra were recorded at 4 K.

DISCUSSION

Heme Ligation State in the Heme A-Apo-Mb Complex

The incorporation of heme A into apo-Mb produces a protein-porphyrin complex which exhibits spectroscopic properties corresponding to both high- and low-spin heme configurations at room temperature. The optical absorption spectrum of the ferric heme A-apo-Mb complex displays features in the visible region (591 nm and 640 nm) which are similar to those observed in the visible absorption spectrum obtained by summing the individual absorption spectra of the ferric high-spin heme A bis-DMSO complex and that of the ferric low-spin

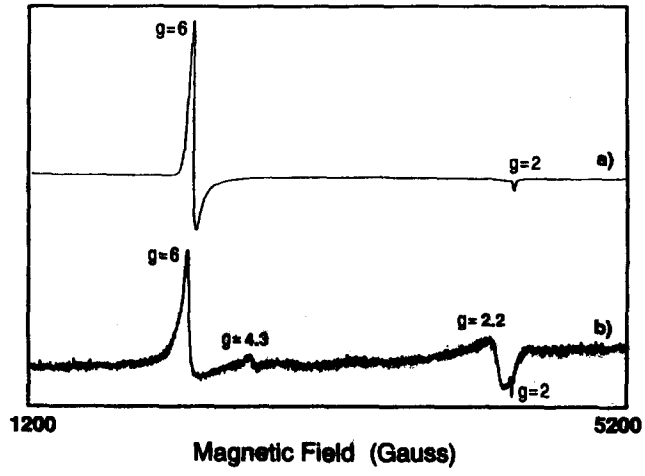

FIGURE 6. Low-temperature EPR spectra of (a) native ferric Mb and (b) ferric heme A-apo-Mb complex. All spectra were recorded at 4 K. Sample concentration was 100 μM for the ferric heme A-apo-Mb complex and 250 μM for native ferric Mb. Other spectral conditions were: microwave power, 2 mW; field modulation, 10 gauss; time constant, 0.064 sec; scan time 4 min.

heme A bis-imidizole complex (587 nm and 640 nm). In addition, the Soret absorption band of the ferric high-spin heme A-apo-Mb complex is in a position intermediate between that of the ferric heme A bis-DMSO (410 nm) and that of the ferric low-spin heme A bis-imidizole (424 nm) complexes. The corresponding bandwidth of the Soret band in the spectrum of the ferric heme A-apo-Mb complex ($\Delta\lambda_{1/2}$ of 45 nm) is considerably broadened relative to the bandwidths of the individual Soret bands of the ferric heme A model complexes ($\Delta\lambda_{1/2}$ of 30 nm) but is similar to the bandwidth of the Soret band in the spectrum resulting from the summation of the Soret bands of the ferric heme A model complexes ($\Delta\lambda_{1/2}$ of 40 nm).

The high-frequency resonance Raman spectra of both the ferric and ferrous forms of the heme A-apo-Mb complex display vibrational bands in the spin-state sensitive region of the spectrum (< 1440 cm^{-1}) which provide further support for the assignment of multiple spin-states in this complex. Previous studies by Choi et al. [15] and Parthasarathi et al. [16] have shown that both ν_2 (1550–1590 cm^{-1}) and ν_3 (1450–1510 cm^{-1}) exhibit a linear dependence on porphyrin core-size. The resonance Raman spectrum of the ferric heme A-apo-Mb complex displays pronounced intensity in the ν_3 region of the spectrum at 1505 cm^{-1} with a low-frequency shoulder at 1490 cm^{-1}. The resonance Raman spectrum of the corresponding ferrous heme A-apo-Mb complex exhibits two bands of equal intensity at 1465 cm^{-1} and 1490 cm^{-1}. Previous resonance Raman studies of heme A model compounds [14, 15] and yeast cytochrome c peroxidase [17] have shown that the bands located at 1505 cm^{-1} (ferric heme A-apo-Mb complex) and 1490 cm^{-1} (ferrous heme A-apo-Mb complex) correspond to 6-coordinate low-spin heme while the bands found at 1490 cm^{-1} (ferric heme A-apo-Mb complex) and 1465 cm^{-1} (ferrous heme A-apo-Mb complex) are indicative of a 5-coordinate high-spin complex. The presence of two bands in the ν_2 region of the resonance Raman spectra of the ferric heme A-apo-Mb complex (1588 cm^{-1} and 1570^{-1}) parallel the ν_3 region with the 1588 cm^{-1} assigned to low-spin heme and the 1570 cm^{-1} representing the high-spin contribution [16].

In contrast to the room temperature optical and resonance Raman spectra, the low-temperature EPR spectrum of the ferric heme A-apo-Mb complex displays a strong $g = 6$ resonance, associated with a high-spin heme Fe. Little or no intensity is observed in low-spin, $g = 3$ region. The appearance of predominantly high-spin EPR resonances in the ferric heme A-apo-Mb complex indicates that the distribution of spins consists of a thermodynamic equilibrium between a high- and low-spin heme. Since the ground-state configuration is high-spin, it is unlikely that the spin equilibrium is due to the lowering of the crystal field splitting energy of the heme Fe. A more likely circumstance involves temperature-dependent ligand binding to the sixth position of the heme A Fe. This scenario is analogous to previous studies on cytochrome c peroxidase where temperature-dependent resonance Raman measurements indicate a similar spin equilibrium arising from changes in heme axial ligation brought about by freezing-induced conformational transitions [17]. The nature of the structural perturbations that might be responsible for the onset of the spin equilibrium in the heme A-apo-Mb complex is discussed below.

The nature of the proximal ligand in the heme A-apo-Mb complex is difficult to ascertain. The low-frequency region of the resonance Raman spectrum of the ferrous heme A-apo-Mb complex does not display significant intensity in the

$\nu_{Fe\text{-}His}$ stretching region (200–250 cm^{-1}). This may arise from a decrease in resonance enhancement of the high-spin ferrous heme A-apo-Mb complex due to excitation at 440 nm. At this wavelength, the extinction of the low-spin ferrous heme A-apo-Mb complex is greater than that of the corresponding high-spin ferrous heme A-apo-Mb complex. On the other hand, both the optical absorption and EPR spectra of the azide-bound ferric heme A-apo-Mb complex (data not shown) are indicative of a low-spin heme chromophore, suggesting that the heme A chromphore is coordinated to a strong-field proximal ligand (presumably the proximal hisitidine) in the reconstituted complex. Bis-azide heme complexes are known to be predominantly high-spin.

Heme A Peripheral Environment

The high-frequency resonance Raman spectra of the heme A-apo-Mb complex above 1600 cm^{-1} is of particular interest since this region contains the vibrational mode assignable to a symmetric $-C{=}O$ vibration of the formyl side chain of heme A. The position of the $\nu_{C=O}$ vibrational mode has been previously shown to be sensitive to both metal oxidation state and solvent (protein matrix), thus providing information relating to the peripheral environment of the porphyrin macrocycle [14, 15]. The highest frequency vibrational band in the resonance Raman spectra of the ferric heme A-apo-Mb complex consists of a broad band centered at 1640 cm^{-1} with shoulders at 1600 cm^{-1} and 1675 cm^{-1}. The intense band centered at 1640 cm^{-1} can be assigned to ν_{10} for low-spin heme. The corresponding position of ν_{10} for the high-spin component is located at 1610 cm^{-1}. Thus it is likely that the high frequency shoulders (1660 cm^{-1} and 1675 cm^{-1}) are due to the formyl group of heme A. The ferrous heme A-apo-Mb complex displays intensity at 1610 cm^{-1} and 1630 cm^{-1}. These two bands can be attributed to a combination of ν_{10} for ferrous low-spin heme A (1620 cm^{-1}), ν_{10} for ferrous high-spin heme A (1607 cm^{-1}), $\nu_{C=C}$ for low-spin heme A (1623 cm^{-1}) and $\nu_{C=C}$ for high-spin heme A (1624 cm^{-1}). The only evidence of a formyl vibration in this spectrum is the presence of a high-frequency shoulder on the 1630 cm^{-1} band at 1650 cm^{-1}.

By comparison of these frequencies to those of heme A model compounds in various solvents, it is evident that multiple heme A-apo-Mb species/conformations are present. The highest-frequency bands assigned to the formyl vibrations in both the ferric and ferrous heme A-apo-Mb complexes (1675 cm^{-1} and 1660 cm^{-1}, respectively) are at a position indicative of a subpopulation of heme A in a hydrophobic environment similar to that of ferric cytochrome $\underline{a}_3$ [15]. On the other hand, the lower-frequency band at 1660 cm^{-1} in the ferric heme A-apo-Mb complex indicates the presence of heme A in a more hydrophilic environment. This assignment of the 1660 cm^{-1} band in the ferric heme A-apo-Mb complex is based upon earlier work [15] showing that the position of the formyl vibrational mode is sensitive to the solvent environment of heme A model compounds and can shift as much as 20 cm^{-1} to lower frequency upon hydrogen bonding.

Origins of the Structural Perturbations in the Heme A-apo-Mb Complex

It is apparent from the spectroscopic data presented here that multiple conformations are present in the heme A-apo-Mb complex, at least two of which are spectroscopically distinct (a high-spin heme complex which is spectroscopically

similar to native Mb and a low-spin heme complex). These structural perturbations in the heme A-apo-Mb complex most certainly arise from the refolding of the apo-Mb around the heme A chromophore. Previous studies utilizing both ^{1}H NMR spectroscopy and x-ray crystallography indicate that the primary forces governing protein folding about the heme group in Mb involves both hydrophobic contacts between the porphyrin and hydrophobic amino acids associated with the interior of the protein and electrostatic interactions between the propionic acid side-chains of the porphyrin and hydrophilic amino acids near the protein exterior [5, 7]. Specifically, the heme b of native Mb forms hydrophobic contacts between the vinyl groups at positions 2 and 4 of the porphyrin and Val E11, Ile FG5, and Phe CD1 located in the interior of the Mb while electrostatic interactions occur between the propionic acid side-chains and His FG3 and Arg CD3 located at the protein surface.

Hauksson et al. [5] have suggested that the initial events in the refolding of apo-Mb around heme b involve electrostatic contacts. This nucleation is then stabilized by hydrophobic contacts. Presumably the initial events in the refolding of apo-Mb around heme A would parallel those of the apo-Mb-heme b system. However, the secondary events involving the hydrophobic interactions are likely to be considerably perturbed by the presence of the long hydrophobic side-chain of the heme A moiety. By orienting the hydrophobic tetradecatrienyl group at position 2 of heme A toward the interior of the apo-Mb, significant disruption of the hydrophobic contacts between the helices which form the "back-side" of the heme pocket (F-, G- and H-helices) would occur. Such disruptions could significantly affect the position of the E-helix and allow the distal histidine (His E7) to move into thermodynamic contact with the heme. This scenario is consistent with the thermodynamic distribution of heme A spin-states observed in the heme A-apo-Mb complex.

CONCLUSION

The data presented here indicate that the incorporation of heme A into apo-Mb causes significant perturbations in the refolding of the apo-Mb about the heme group. This is most evident by the apparent thermodynamic distribution of high- and low-spin heme configurations in the heme A-apo-Mb complex. Further evidence of structural perturbations in this complex is provided by the presence of multiple formyl stretching vibrations which indicate that a distribution of both hydrophobic and hydrophilic heme peripheral environments are present. This study demonstrates that specific constraints must be placed upon the structure of the heme pockets of cytochrome c oxidase to accommodate the unusual stereochemistry of heme A.

We are grateful to Dr. Barry B. Muhoberac (Indiana University—Purdue University at Indianapolis) for helpful and enlightening discussions during the course of this work.

This work is contribution No. 8505 from the Arthur Amos Noyes Laboratory of Chemical Physics, California Institute of Technology, Pasadena, California. We were supported by grants No. GM22432 (SIC) and No. GM33330 (MRO) from the National Institute of General Medical Sciences, U.S. Public Health Service and grant No. PRF19671-AC3 (SIC) from the Petroleum Research Fund of the American Chemical Society.

REFERENCES

1. M. Wikstrom, K. Kraab, and M. Saraste, *Cytochrome Oxidase: A Synthesis*, Academic Press, London and New York, 1981.
2. W. S. Caughey, G. A. Smythe, D. H. O'Keefe, J. E. Maskasky, and M. L. Smith, *J. Biol. Chem.* **250**, 7602 (1975).
3. P. M. Callahan and G. T. Babcock, *Biochemistry* **22**, 452, (1983).
4. W. H. Woodruff, R. J. Kessler, N. S. Ferris, and R. F. Dallinger, *Electron Transfer and Oxygen Utilization* C. Ho, Ed., Elsevier/North Holland, New York, 1982, pp. 191–198.
5. J. B. Hauksson, G. N. La Mar, R. K. Pandey, I. N., Rezzano, and K. M. Smith, *J. Amer. Chem. Soc.* **112** 8315 (1990).
6. M. Tsubaki, K. Nagai, and T. Kitagawa, *Biochemistry* **19**, 379 (1980).
7. K. Miki II, M. Yukawa, A. Owatari, Y. Hato, S. Harada, Y. Kai, N. Kasai, Y. Hata, N. Tanaka, M. Kakudo, Z. Katsube, K. Kawabe, Z. Yoshida, and H. Ogashi, *J. Biochem.* **100**, 269 (1986).
8. M. B. Steup and B. B. Muhoberac, *J. Inorg. Biochem* **37**, 233 (1989).
9. R. F. R. S. Lemberg, D. B. Morell, N. Newton, and J. E. O'Hagen, *Proc. Royal Soc.* (London) Ser. B 155, 339 (1961).
10. C. R. Hartzell and H. Beinert, *Biochim. Biophys. Acta* **368**, 318 (1974).
11. S. Takemori and T. E. King, *J. Biol. Chem.* **240**, 504 (1965).
12. F. W. J. Teal, *J. Biol. Chem.* **35**, 543 (1959).
13. R. W. Larsen, *Dissertation*, University of New Mexico, 1990.
14. G. T. Babcock, *Biological Applications of Raman Spectroscopy*, T. G. Spiro, Ed., Wiley and Sons, New York, 1988, Vol. 3.
15. S. Choi, J. J. Lee, Y. H. Wei, and T. G. Spiro, *J. Am. Chem. Soc.* **105**, 3692 (1983).
16. N. Parthasarathi, C. Hansen, S. Yamaguchi, and T. G. Spiro, *J. Am. Chem. Soc.* **109**, 3865 (1987).
17. G. Smulevich, A. R. Mantini, A. M. English, and J. M. Mauro, *Biochemistry* **28**, 5058 (1989).

Received September 23, 1991; accepted January 9, 1992